Fluorescent Hydroxyapatite-Loaded Biodegradable Polymer Nanoparticles with Folate Decoration for Targeted Imaging

Jie Pan, Dong Wan, and Yuxia Bian
State Key Laboratory of Hollow Fiber Membrane Materials and Processes, Department of Pharmaceutical Engineering, School of Environmental and Chemical Engineering, Tianjin Polytechnic University, Tianjin 300387, China

Hongfan Sun and Chao Zhang
Tianjin Key Laboratory of Biomaterial Research, Institute of Biomedical Engineering, Peking Union Medical College and Chinese Academy of Medical Sciences, Tianjin 300192, China

Fengmin Jin
School of Chemical Engineering and Technology, Tianjin University, Tianjin 300072, China

Zhiqi Huang and Jinlong Gong
Key Laboratory for Green Chemical Technology of Ministry of Education, School of Chemical Engineering and Technology, Tianjin University, Tianjin 300072, China

Collaborative Innovation Center of Chemical Science and Engineering, Tianjin 300072, China

DOI 10.1002/aic.14210
Published online August 12, 2013 in Wiley Online Library (wileyonlinelibrary.com)

The preparation of the luminescent hydroxyapatite (HAP)-loaded biocompatible nanoparticles (NPs) for targeted imaging of cancer cells is described. Currently, cellular imaging using fluorescent probes is an important technique for the early diagnosis of cancer. Compared with the quantum dots, luminescent HAP is a new fluorescent material with many advantages such as low toxicity, biocompatibility, thermal stability, resistance to erosion, and low prices. Thus, luminescent HAP has enormous potential to be used as biological fluorescent probes. However, luminescent HAP is water-insoluble, low sensitivity, which limit its application in the field of cellular imaging. Surface modification of NPs with targeting molecule was carried out to achieve its target function. Thus, novel fluorescent NPs with low toxicity, high sensitivity, and good photostability were prepared to be used for targeted imaging of cancer cells. This study initially explored the applications of luminescent HAP in the field of targeted cellular imaging. This NPs platform will be a promising tool for molecular imaging and medical diagnostics, especially the detection of cancer at its early stage.
 AIChE J, 59: 4494–4501, 2013
Keywords: cancer cells, cellular imaging, nanoparticles, cellular imaging, Eu-hydroxyapatite

Introduction

As a report from the American Cancer Society, cancer is a major public health problem in the world. According to a report from American Cancer Society, a total of 1,638,910 new cancer cases and 577,190 deaths will be due to cancer in the United States in 2012. During past decades, the development of nanoparticles (NPs), which provided exciting possibilities in biomedical fields, received much attention from researchers. It was reported that global market related with the applications of nanotechnology in the medical field could increase to about $70–160 billion by 2015.[1]

To efficiently prevent and treat cancer, it is crucial to develop new technologies to realize early investigation, early diagnosis, and consequent early treatment about cancer. Technology of cellular imaging can intuitively characterize normal and pathological changes in organisms at the cellular and molecular level. Therefore, this technology can be used for dynamic monitoring some of the key single-molecule events and cancer metastasis in the process of tumor occurrence and development, and reveals cancer occurrence, development, and transfer mechanisms. Thus, cellular imaging is expected to provide a more effective tool for the early diagnosis of cancer, carcinogenic mechanisms, and evaluation of treatment on cancer.[2]

Quantum dots (QDs) are received more concern as luminescence probes in the fields of cellular imaging recent decades. In comparison to conventional dyes, QDs show various and unique advantages in optical and chemical properties such as tunable emission from visible to infrared wavelengths by changing their size and composition, broader excitation spectra due to high absorption coefficients, high-quantum yield of fluorescence, strong brightness, photostability, and high resistance to photobleaching.[3–5] These unique

Correspondence concerning this article should be addressed to J. Gong at jlgong@tju.edu.cn.

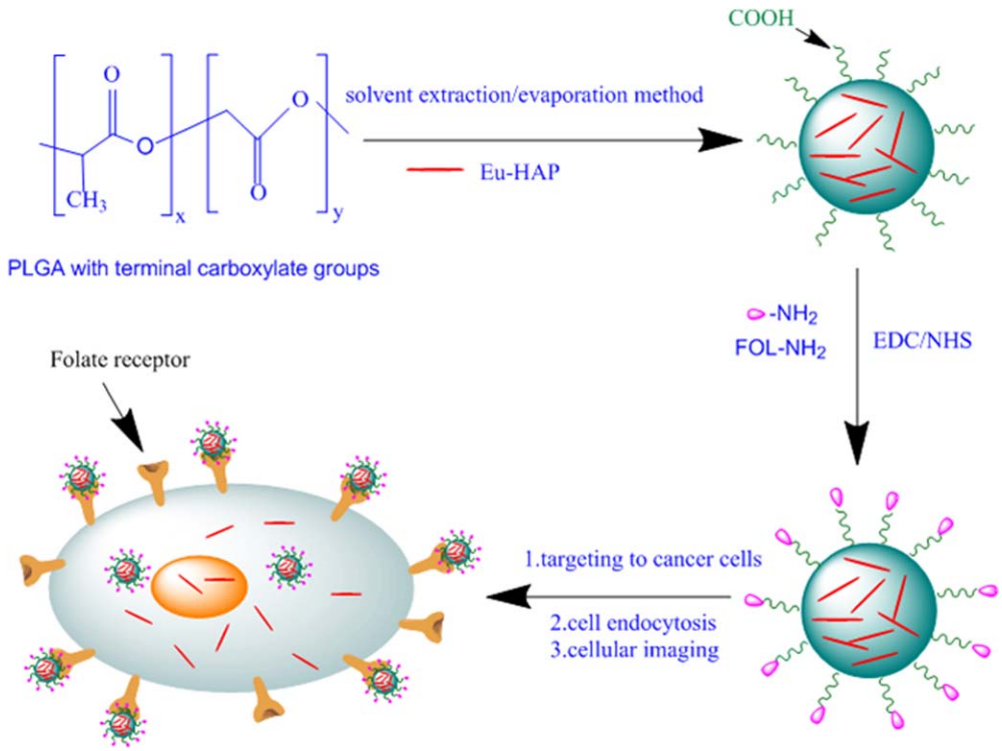

Figure 1. Detailed scheme about preparation of Eu-HAP-loaded NPs with folate decoration for cellular imaging.

[Color figure can be viewed in the online issue, which is available at wileyonlinelibrary.com.]

properties of QDs have attracted tremendous interest in exploiting them in a variety of biological field. But toxic effects of QDs, which result from oxidative degradation of the heavy metal components in QDs, limit their applications in the fields of biology and medicine.[6–8] Although some literatures in recent years reported that the toxicity of QDs can be decreased to some extent through surface modification or encapsulated in biodegradable nanospheres,[9–14] the toxic problem of QDs is still not fundamentally solved. Therefore, it is urgent to found a new fluorescent material with low toxicity, high biocompatible, strong fluorescent intensity, and steady luminescent property to replace with QDs.

Hydroxyapatite (HAP) is the main inorganic component of bones and teeth of humans and animals, and it has good biocompatibility, and highly stable *in vivo*.[15–17] Because HAP itself does not have the fluorescent property, the development of luminescent HAP is a key issue for applications of HAP in cellular imaging. Wang et al. successfully prepared luminescent Eu^{3+}-doped HAP (Eu-HAP), which promotes the prospect of Eu-HAP used in cellular imaging. Compared to a conventional organic fluorescent dyes and QDs, Eu-HAP show many merits such as low toxicity, high fluorescent intensity, high photostability, biocompatibility, anticorrosion, and a low price.[17] These luminescent HAPs as fluorescent probes have been successfully applied in cellular imaging.[18,19] Therefore, Eu-HAP as a new type of fluorescent material has as a great potential to be applied as biological fluorescent probe.

However, the Eu-HAPs have several defects such as insufficient water solubility and low sensitivity and so on, which limit their application in the field of cellular imaging. These limitations can be solved through encapsulation of Eu-HAP in biocompatible polymer (such as Poly(D,L-lactide-co-glycolide), PLGA) NPs with targeting molecule (such as folate). Folic acid (folate) is an attractive target ligand because of its high binding affinity for the folate receptors ($K_d \sim 10^{-10}$ M).[20,21] Folate and its conjugates have been widely used for selective delivery of anticancer agents to cells with folate receptor, which are overexpressed in many kinds of human cancer cells such as ovarian, breast, and prostate cancers while only minimally distributed in normal tissues.[22–26]

In this study, Eu-HAP-loaded PLGA NPs with folate decoration were prepared to enable Eu-HAP water-soluble, increase biocompatibility and stability of Eu-HAP and improve imaging specificity, sensitivity of cancer cells through selective delivery of Eu-HAP to appropriate tumor cell lines. This NPs platform will promote revolution of cellular imaging and medical diagnostics, especially the cancer detection at its early stage. The detailed scheme for the preparation of folate-decorated (FD) Eu-HAP-loaded NPs for cellular imaging is shown in Figure 1.

Materials and Methods

Materials

Eu-HAP was synthesized according to the literature.[17] Poly(D,L-lactide–*co*–glycolide) (50/50) with terminal carboxylate groups (PLGA MW: 38,000–54,000), 3-(4,5-dimethylthiazol-2-yl)−2,5-diphenyl tetrazolium bromide (MTT), penicillin-streptomycin solution, Trypsin-EDTA solution, *N*,*N*′-dicyclohexylcarbodiimide (DCC), 4-dimethylamino pyridine, 1-ethyl-3-(3-dimethylaminopropyl) carbodiimide hydrochloride (EDC), *N*-hydroxysuccinimide (NHS), glutaric acid, folic acid, pyridine, and poly(vinyl alcohol) (PVA) (MW: 30,000–70,000) were purchased from Sigma-Aldrich (St. Louis, MO). Fetal bovine serum (FBS) was purchased from Gibco (Life Technologies AG, Switzerland). Roswell Park Memorial Institute (RPMI) 1640 medium without folic acid was from Invitrogen Corporation. Millipore water was produced

by the Milli-Q Plus System (Millipore Corporation, Bedford, MA). MCF-7 breast cancer cells were provided by American Type Culture Collection.

Fabrication of NPs

The Eu-HAP-loaded NPs were prepared by a modified solvent extraction/evaporation single-emulsion method. In a brief, 0.5 mg Eu-HAP and 50 mg PLGA were dissolved in 4 mL dichloromethane (DCM), and then this solution was poured gradually into 60 mL aqueous phase containing 0.5 % (w/v) PVA as emulsifier under gentle stirring. Next, the mixture was sonicated for 120 s at 25 W output. The resultant emulsion was stirred overnight at room-temperature to evaporate organic solvent (DCM). The suspension of resulting NPS was centrifuged at 10,500 rpm for 15 min to obtain the NPs in the pellet. After the NPs were washed twice with deionized (DI) water, the NPs powder was further obtained after freeze-drying for 2 days. The same procedure as for the preparation of Eu-HAP NPs was exploited to design pure Eu-HAP NPs without the PLGA matrix, a DCM solution (1 mL) containing 0.5 mg of Eu-HAP was poured into 60 mL of PVA aqueous solution.

Formulation of Eu-HAP-loaded NPs with folate-decoration

The amination of folic acid (folate) was first synthesized following the procedure in the literature.[27] Briefly, folic acid was reacted with DCC and NHS in DMSO at stoichiometric molar ratio of folic acid/DCC/NHS = 1/1.2/2 for 6 h at 50°C. This activates the folic acid was allowed to react with ethylene diamine with pyridine as catalyst. Excess acetonitrile was added to precipitate out folate-NH_2, and was collected by vacuum filtration.

The Eu-HAP-loaded NPs with folate-decoration were prepared as follows: 10 mg NPs were resuspended in 5 mL DI water to give a concentration of 2 mg/mL and placed in an ultrasonic bath to disperse the NPs. After addition of EDC (0.32 mg) and NHS (0.36 mg), the surface carboxyl groups of Eu-HAP-loaded PLGA NPs were activated for 2.5 h at room-temperature. Borate buffer (5 mL, 0.2 M, pH = 8.5) was then added to the suspension, which was followed by the addition of 0.1mL of aminated folic acid (0.1 M) in DMSO solution. After the reaction was allowed to take place for 4 h at room-temperature, the mixture was then washed and centrifuged with DMSO and DI water to remove unreacted folate-NH_2. The eventual NPs product obtained was collected by freeze-drying.

Characterization of NPs

Particle Size and Size Distribution. Average particle size and size distribution of the Eu-HAP-loaded NPs with or without folate-decoration were measured using laser light scattering (LLS, 90 Plus Particle Size, Brookhaven Instruments, USA). The NPs were diluted with DI water and sonicated for 2 min before measurement. The homogeneous suspension was used to determine the volume mean diameter, size distribution, and polydispersity.

Surface Charge. Zeta potential of NPs was determined with ZetaPlus zeta potential analyzer (Brookhaven Instruments Corporation) at room-temperature. The samples were prepared by diluting the NPs suspension with DI water.

Surface Morphology. The shape and surface morphology of NPs were studied with transmission electron microscope (TEM, JEM-2010F, JEOL, Japan). NPs suspension was dropped on the surface of copper grid with carbon film and dried at room-temperature.

Emission Spectrum. Suspension solutions of NPs were placed into a quartz cuvette. Emission spectrum was recorded with spectrofluorophotometer (RF-5301PC, SHIMADZU, Japan) at excitation 405 nm.

Eu-HAP Encapsulation and Loading Efficiency. The encapsulation efficiency of the Eu-HAP in the NPs was investigated with spectrofluorophotometer (RF-5301PC, SHIMADZU, Japan). In a brief, 1 mL suspension solution of NPs was freeze-dried, and then redissolved in 1 mL DCM for the emission analysis. The emission at 516 nm under excitation at 405 nm was measured to determine the Eu-HAP content in the solution with a previously established calibration curve.

$$\text{Eu-HAP Encapsulation Efficiency}\,(\%) = \frac{\text{Encapsulated amount of Eu-HAP in NPs}}{\text{Total amount of Eu-HAP added in the process}} \times 100\%$$

Cell line experiment

Cell Cultures. MCF-7 breast cancer cells and NIH 3T3 fibroblasts were cultured in folate-free RPMI 1640 medium supplemented with 10% FBS and 1% antibiotics. Cells were cultivated in medium at 37°C in humidified environment of 5% CO_2. Before the *in vitro* experiments, the cells were pre-cultured until confluence was reached.

In Vitro *Cellular Uptake of NPs.* To evaluate the targeting efficacy of Eu-HAP loaded NPs with or without folate decoration, the *in vitro* cellular uptake of NPs were carried out.

For qualitative study, MCF-7 cells were cultured in chamber (LAB-TEK, Chambered Coverglass System) at 37 °C. After 80% confluence, the medium was removed, and the adherent cells were washed twice with PBS buffer. And 0.6 mL of Eu-HAP-loaded NPs with or without folate decoration diluted in the medium at 3.1 μg/mL Eu-HAP concentration was added into the chamber. After incubation for 2.5 and 4 h, the cells were washed four times with PBS. Next, they were fixed by 75% ethanol for 15 min. The cells were washed twice with PBS and observed using confocal laser scanning microscopy (CLSM; Zeiss LSM 410, Jena, Germany). The images of the Eu-HAP were recorded with red channel (excitation at 405 nm).

For quantitative study, MCF-7 were seeded into 96-well black plates (Costar, IL) at 1×10^4 cells/well. After cells reached 80% confluence, the medium was changed with suspension of the Eu-HAP-loaded NPs with or without folate decoration in folate-free RPMI 1640 medium at 6.2 μg/mL Eu-HAP concentration. After incubation for 2.5 and 4 h, the NPs suspension was removed, and the wells were washed with 50 μL of PBS for three times to remove traces of NPs. Furthermore, 100 μL of fresh medium was then added to each sample well followed by addition of 50 μL of 0.5% Trition X-100 in 0.2 N NaOH to lyse the cells. The fluorescence intensity of each sample well was determined with microplate reader (Genios, Tecan, Männedorf, Switzerland) with excitation wavelength at 405 nm and emission wavelength at 516 nm. The cellular uptake efficiency was expressed as the percentage of sample well fluorescence vs. that of the positive control solution.

In vitro Cytotoxicity of Eu-HAP-Loaded NPs. To investigate the cytotoxicity of Eu-HAP-loaded NPs, MTT assay

Table 1. Characteristics of Eu-HAP-Loaded NPs With or Without Folate Decoration at Various Blend Ratio ($n = 6$)

NPs	Particle Size (nm)	Polydispersity	EE (%)	Zeta Potential (mV)
NPs without folate decoration	250.2 ± 8.6	0.137 ± 0.051	46.8	-22.4 ± 2.2
NPs with folate decoration	253.5 ± 6.1	0.121 ± 0.025	45.1	-20.1 ± 1.6

were exploited. NIH 3T3 fibroblast cells were incubated in 96-well plates (Nunc, Roskilde, Danmark) at an intensity of 40,000 cells/mL. After 48 h seeding, the old medium was replaced with Eu-HAP-loaded NPs or pure Eu-HAP NPs containing medium at Eu-HAP concentration of 0.0032, 0.032, 0.32, and 3.2 μg/mL. At designated time intervals (12, 24, and 48 h), cell viability were determined with MTT assay. After 4 h incubation with MTT supplemented with 90 μL culture medium, the medium was removed and the purple crystals were dissolved with isopropanol. The fluorescence intensity of the cells was measured using the microplate reader (Genios, Tecan, Männedorf, Switzerland). The absorbance wavelength was set at 570 nm and background wavelength at 660 nm. Cell viability was calculated using the following equation.

$$\text{Cell viability } (\%) = \frac{\text{Int}_s}{\text{Int}_{\text{control}}} \times 100$$

Where Int_s is the fluorescence intensity of the cells incubated with the NPs suspension and $\text{Int}_{\text{control}}$ is the fluorescence intensity of the cells incubated with the culture medium only.

Results and Discussion

Characterization of Eu-HAP-loaded NPs with folate decoration

Size Distribution. Table 1 show the size and the size distribution of Eu-HAP-loaded NPs with or without folate decoration measured using LLS. The average diameter of fabricated NPs with folate decoration ranged between 247 and 260 nm. It is noticed in the Table 1 that there is no significant change in the size of NPs with or without folate.

Surface Charge. The value of zeta potential is crucial for maintaining the colloidal stability of NPs suspension. NPs with higher electric charge on their surface demonstrate good colloidal stability in solution due to enhanced electrostatic repulsion among particles.[28] As shown in Table 1, the Eu-HAP-loaded NPs with folate decoration were ~ -20.1 mV, which indicate fabricated NPs are stable in suspension.

Surface Morphology. Figure 2 show TEM image of Eu-HAP-loaded NPs with folate decoration, it can be seen that the NPs are dispersed as individual NPs with a well-defined spherical shape and homogeneously distributed around 200 nm in diameter (Figures 2A, B). And also it can be observed that several Eu-HAPs (seen as dark bar, ~100 nm) were encapsulated completely in interior of one PLGA NPs (seen as brighter circle, ~200 nm). Furthermore, no aggregation was observed, and the incorporation of Eu-HAP into NPs did not seem to cause morphological changes. Moreover, it was found that the particle size (~200 nm) observed from TEM images is small in comparison with that (~250 nm) determined by LLS, which is maybe due to the shrinkage of the polymeric NPs during the sample preparation in vacuum.[29] HRTEM image taken from single sphere indicates that the encapsulated Eu-HAP nanocrystals are still highly crystalline (Figures 2C, D). Elemental mapping show the even distribution of the main elements in the spheres (Figure 3).

Emission Spectra. The emission spectrum of the Eu-HAP-loaded NPs with or without folate decoration in water and Eu-HAP in DCM were demonstrated in Figure 4. From this figure, it can be seen that there is almost no different the full width at half-maximum for Eu-HAP-loaded NPs with or without folate decoration in water and Eu-HAP in DCM, and only small shift of peak appeared (emission peak at 516 nm for Eu-HAP-loaded NPs with folate decoration in water, 519 nm for Eu-HAP in DCM, and 520 nm Eu-HAP-loaded NPs in water, respectively), which confirm that the process of preparing NPs and following folate decoration did not effect on the fluorescent properties of Eu-HAP.

Eu-HAP Encapsulation Efficiency. As shown in Table 1, the Eu-HAP encapsulation efficiency in the PLGA NPs with folate decoration is 45.1%, which confirmed that developed NPs in this study demonstrated high loading capacity for Eu-HAP. This high payload of Eu-HAP in NPs benefits to enhance the capability of the NPs to produce bright fluorescence in a biological field.

In Vitro Cellular Uptake of NPs. CLSM was used to investigate cellular uptake efficiency of MCF-7 cells treated with NPs, which can evaluate the application of NPs for cellular imaging. Figure 5 demonstrated the CLSM images of MCF-7 cells treated with (A) Eu-HAP-loaded NPs without folate decoration, (B) Eu-HAP-loaded NPs with folate decoration after 2.5 h incubation; and (C) Eu-HAP-loaded NPs without folate decoration (D) Eu-HAP-loaded NPs with folate decoration after 4 h incubation at 3.1 μg/mL Eu-HAP concentration at 37°C. Here, CLSM images were obtained under the excitation at 405 nm, and red channel shows the fluorescence images of Eu-HAP.

As shown in CLSM images, the fluorescence of FD NPs in the cells (Column 2) are much brighter than that of the NPs without folate decoration (Column 1), which demonstrated that the FD NPs demonstrated higher cellular uptake efficiency by MCF-7 cancer cells than that of NPs without folate decoration at same incubation time (2.5 and 4 h) and Eu-HAP's concentration. Perhaps, this phenomenon is due to a high level of folate receptor on the surface of MCF-7 breast cancer cells, which can be targeted by FD NPs. Consequently, more FD NPs were internalized by MCF-7 cancer cells via folate receptor-medicated endocytosis than NPs without folate decoration. These findings prove strongly that FD NPs can be used efficiently for targeted cellular imaging.

The experiments on quantitative cellular uptake of NPs by MCF-7 cancer cells were also performed to further confirm the targeting effect of FD NPs. In Figure 6, FD NPs expressed 1.27- and 1.39-fold higher cellular uptake efficiency than NPs without folate decoration after 2.5 and 4.0-h incubation with MCF-7 cells, respectively, because the MCF-7 cancer cells have overexpression of folate receptors on their surface. The results in Figure 6 matched completely

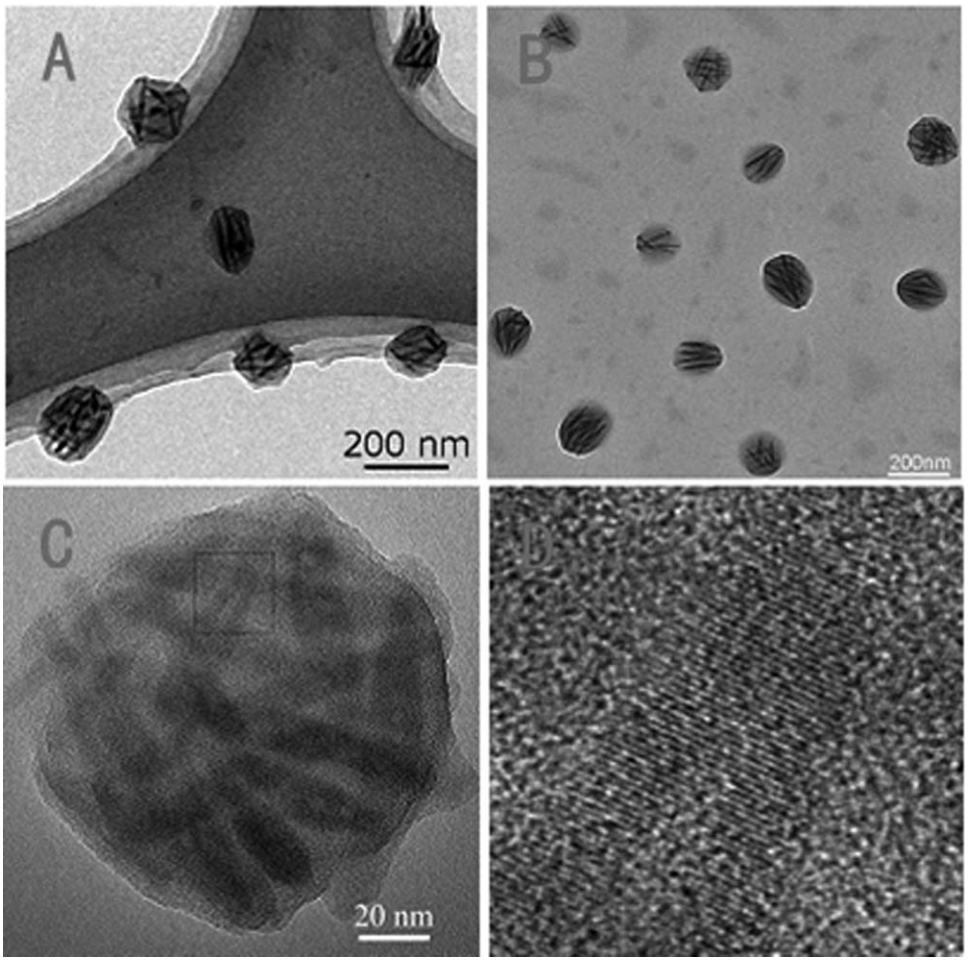

Figure 2. (A and B) TEM image of Eu-HAP-loaded NPs with folate decoration; (C) HRTEM images of a single Eu-HAP polymer NP; (D) enlarged HRTEM image of the square part in Fig. 2C.

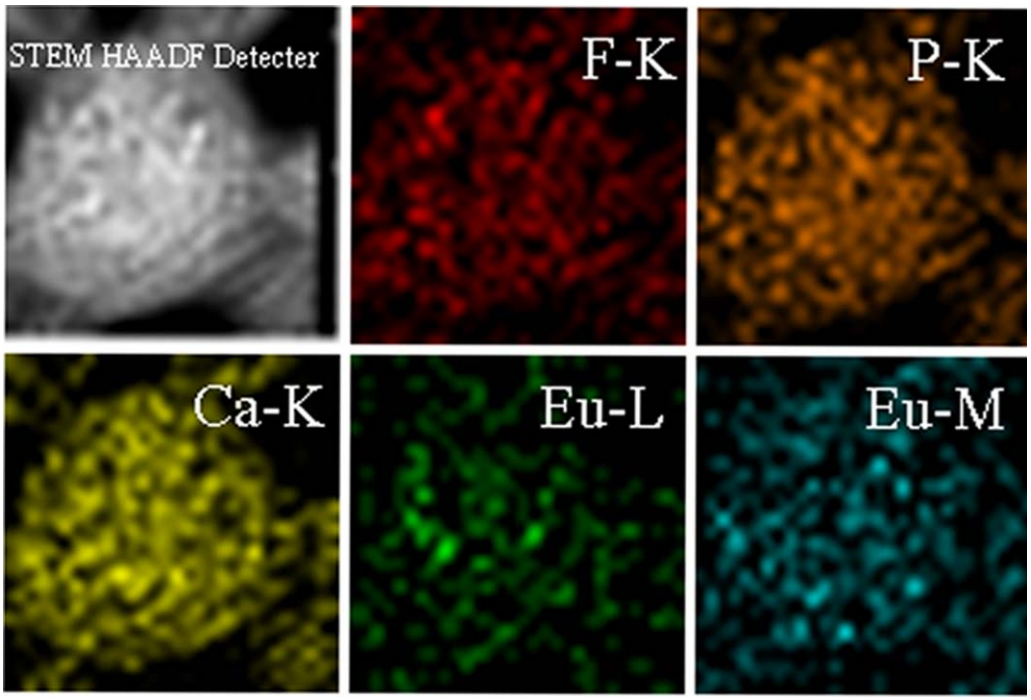

Figure 3. Elemental mapping of a single-Eu-HAP polymer NP showing the coexistence of F, P Ca, and Eu elements.

[Color figure can be viewed in the online issue, which is available at wileyonlinelibrary.com.]

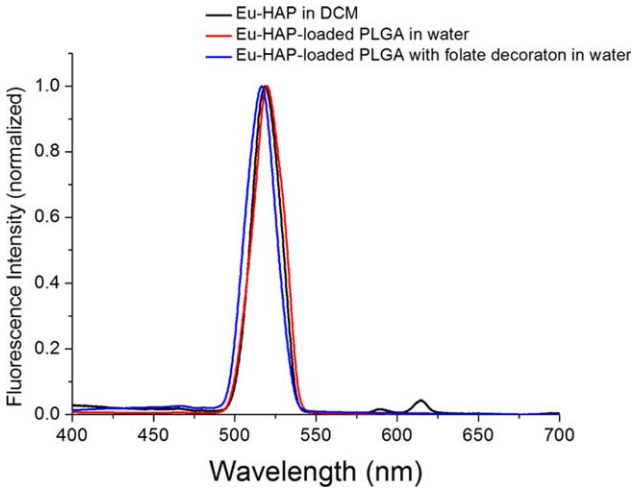

Figure 4. Emission spectrum of Eu-HAP in DCM and Eu-HAP-loaded NPs with or without folate decoration in water at excitation 405 nm.

[Color figure can be viewed in the online issue, which is available at wileyonlinelibrary.com.]

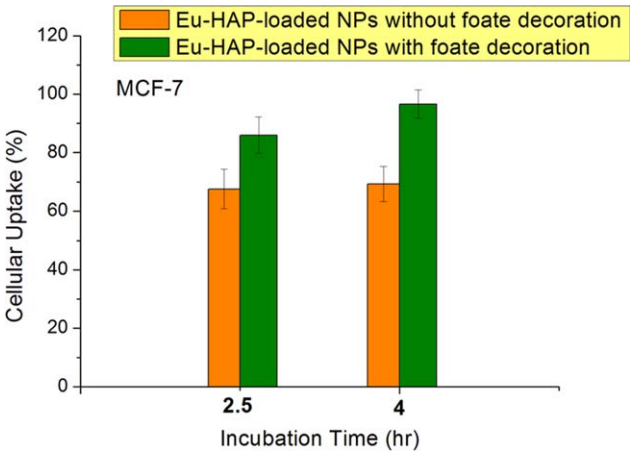

Figure 6. MCF-7 cells uptake efficiency of Eu-HAP-loaded NPs with or without folate decoration in medium at the Eu-HAP concentration of 6.2 μg/mL for 2.5 and 4.0 h, respectively ($n = 6$).

[Color figure can be viewed in the online issue, which is available at wileyonlinelibrary.com.]

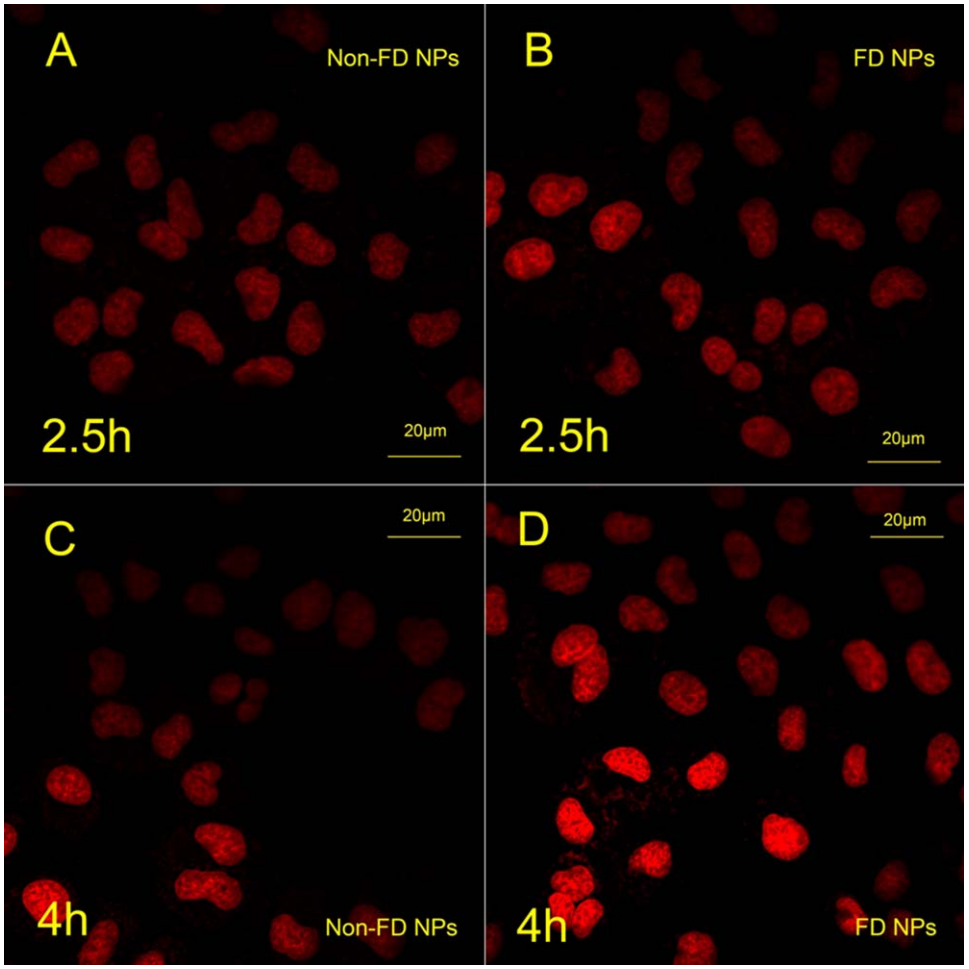

Figure 5. Confocal laser scanning microscopy of MCF-7 cells treated with (A) Eu-HAP-loaded NPs without folate decoration, (B) Eu-HAP-loaded NPs with folate decoration after 2.5-h incubation; and (C) Eu-HAP-loaded NPs without folate decoration (D) Eu-HAP-loaded NPs with folate decoration after 4-h incubation at 3.1-μg/mL Eu-HAP concentration at 37°C.

[Color figure can be viewed in the online issue, which is available at wileyonlinelibrary.com.]

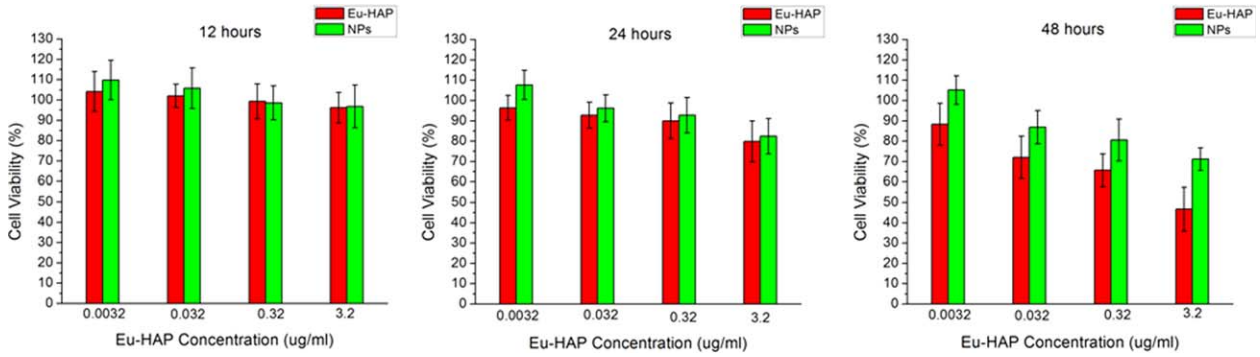

Figure 7. *In vitro* viability of NIH 3T3 cells treated with pure Eu-HAP NPs, Eu-HAP-loaded NPs without folate decoration at the different Eu-HAP concentration after 12, 24, and 48-h culture ($n = 6$).

[Color figure can be viewed in the online issue, which is available at wileyonlinelibrary.com.]

with that in Figure 5, which further illustrates the function of targeted cellular imaging with FD NPs. For FD NPs, the folate receptor-medicated endocytosis can facilitates the cellular uptake, resulting in higher uptake efficiency.

In Vitro Cytotoxicity of Eu-HAP NPs. It was reported that the release of cadmium surface atoms due to surface oxidation of the QDs can lead to the cytotoxicity of QDs, which limit the application of QDs in the biological field.[7] Therefore, it is expected to develop new fluorescent material with less or even no toxicity such as Eu-HAP to replace with QDs. Because Eu-HAP is water-insoluble, encapsulation of Eu-HAP into PLGA NPs can enable Eu-HAP water-soluble. Furthermore, although Eu-HAP NPs has no toxicity, the encapsulation of Eu-HAP into PLGA NPs can further enhance the biocompatibility of Eu-HAP.

To evaluate the cytotoxicity of Eu-HAP NPs, the viability of NIH/3T3 fibroblast cells treated with Eu-HAP-loaded NPs and free Eu-HAP was investigated. Figure 7 illustrates the viability of NIH 3T3 treated with pure Eu-HAP NPs, Eu-HAP-loaded NPs at 0.0032, 0.032, 0.32, and 3.2 μg/mL Eu-HAP concentration after 12, 24, and 48-h culture. The cell viability for Eu-HAP-loaded NPs, which was 96.8 ± 10.5, 82.4 ± 8.7, and $71.1 \pm 5.6\%$, for 12, 24, and 48-h incubation time at 3.2 μg/mL Eu-HAP concentration, respectively, is much lower than that of pure Eu-HAP NPs (96.2 ± 7.4, 79.8 ± 10.0, and $46.8 \pm 10.8\%$). Similar results were also obtained at other Eu-HAP concentration for 12, 24, and 48-h incubation time. This demonstrated that encapsulation of Eu-HAP into PLGA NPs can efficiently minimize the cytotoxicity of Eu-HAP to NIH 3T3 fibroblasts normal cells, which is crucial for the application of Eu-HAP in biological area.

Conclusions

In this study, new Eu-HAP-loaded PLGA NPs with folate decoration were developed for targeted cellular imaging. These Eu-HAP-loaded PLGA NPs with folate decoration are biocompatibility and photostability, and showed specific targeted imaging for MCF-7 breast cancer cells with overexpression folate receptors on their surface via folate receptor-medicated endocytosis. The *in vitro* experiments confirmed the suitability of NPs for biological and medical applications as image generating probes. The fabricated NPs in this study will be a promising tool for various biological applications such as the diagnosis of cancer at its early stage in the future.

Acknowledgments

The authors are grateful for the financial support from National Natural Science Foundation of China (91127040, 20921001, 21222604, and 21172171), the 973 program (2011CB933100), and Natural Science Foundation of Tianjin (No. 11JCZDJC22300). The authors acknowledge the support from the key laboratory of biomedical materials in Tianjin.

Literature Cited

1. Shi J, Votruba AR, Farokhzad OC, Langer R. Nanotechnology in drug delivery and tissue engineering: from discovery to applications. *Nano Lett*. 2010;10:3223–3230.
2. Weissleder R, Mahmood U. Molecular imaging. *Radiology*. 2001; 219:316–333.
3. Michalet X, Pinaud FF, Bentolila LA, Tsay JM, Doose S, Li JJ, Sundaresan G, Wu AM, Gambhir SS, Weiss S. Quantum dots for live cells, in vivo imaging, and diagnostics. *Science*. 2005;307:538–544.
4. Alivisatos AP, Gu W, Larabell C. Quantum dots as cellular probes. *Ann Rev Biomed Eng*. 2005;7:55–76.
5. Smith AM, Duan H, Mohs AM, Nie S. Bioconjugated quantum dots for in vivo molecular and cellular imaging. *Adv Drug Deliv Rev*. 2008;60:1226–1240.
6. Kirchner C, Liedl T, Kudera S, Pellegrino T, Javier AM, Gaub HE, Stölzle S, Fertig N, Parak WJ. Cytotoxicity of colloidal CdSe and CdSe/ZnS nanoparticles. *Nano Lett*. 2005;5:331–338.
7. Derfus AM, Chan WCW, Bhatia SN. Probing the cytotoxicity of semiconductor quantum dots. *Nano Lett*. 2004;4:11–18.
8. Celik A, Comelekoglu U, Yalin S. A study on the investigation of cadmium chloride genotoxicity in rat bone marrow using micronucleus test and chromosome aberration analysis. *Toxicol Ind Health*. 2005;21:243–248.
9. Liu Y, Mi Y, Zhao J, Feng S-S. Multifunctional silica nanoparticles for targeted delivery of hydrophobic imaging and therapeutic agents. *Int J Pharm*. 2011;421:370–378.
10. Muthu MS, Kulkarni SA, Raju A, Feng S-S. Theranostic liposomes of TPGS coating for targeted co-delivery of docetaxel and quantum dots. *Biomaterials*. 2012;33:3494–3501.
11. Pan J, Feng S-S. Targeting and imaging cancer cells by folate-decorated, quantum dots (QDs)-loaded nanoparticles of biodegradable polymers. *Biomaterials*. 2009;30:1176–1183.
12. Pan J, Liu Y, Feng S-S. Multifunctional nanoparticles of biodegradable copolymer blend for cancer diagnosis and treatment. *Nanomedicine*. 2010;5:347–360.
13. Pan J, Wan D, Gong J. PEGylated liposome coated QDs/mesoporous silica core-shell nanoparticles for molecular imaging *Chem Commun*. 2011;47:3442–3444.
14. Pan J, Wang Y, Feng S-S. Formulation, characterization, and in vitro evaluation of quantum dots loaded in poly(lactide)-vitamin E TPGS nanoparticles for cellular and molecular imaging. *Biotechnol Bioeng*. 2008;101:622–633.

15. Palmer LC, Newcomb CJ, Kaltz SR, Spoerke ED, Stupp SI. Biomimetic systems for hydroxyapatite mineralization inspired by bone and enamel. *Chem Rev*. 2008;108:4754–4783.
16. Curtin CM, Cunniffe GM, Lyons FG, Bessho K, Dickson GR, Duffy GP, O'Brien FJ. Innovative collagen nano-hydroxyapatite scaffolds offer a highly efficient non-viral gene delivery platform for stem cell-mediated bone formation. *Adv Mater*. 2012;24:749–754.
17. Hui J, Wang X. Luminescent, colloidal, F-substituted, hydroxyapatite nanocrystals. *Chem Eur J*. 2011;17:6926–6930.
18. Chen F, Huang P, Zhu Y-J, Wu J, Zhang C-L, Cui D-X. The photoluminescence, drug delivery and imaging properties of multifunctional Eu3+/Gd3+ dual-doped hydroxyapatite nanorods. *Biomaterials*. 2011;32:9031–9039.
19. Liu H, Chen F, Xi P, Chen B, Huang L, Cheng J, Shao CW, Wang J, Bai DC, and Zeng ZZ. Biocompatible fluorescent hydroxyapatite: synthesis and live cell imaging applications. *J Phys Chem C*. 2011; 115:18538–18544.
20. Leamon CP, Low PS. Delivery of macromolecules into living cells-a method that exploits folate receptor endocytosis. *Proc Natl Acad Sci USA*. 1991;88:5572–5576.
21. Turek JJ, Leamon CP, Low PS. Endocytosis of folate-protein conjugates-ultrastructural-localization in kb cells. *J Cell Sci*. 1993;106: 423–430.
22. Hilgenbrink AR, Low PS. Folate receptor-mediated drug targeting: from therapeutics to diagnostics. *J Pharm Sci*. 2005;94:2135–2146.
23. Leamon CP, Reddy JA. Folate-targeted chemotherapy. *Adv Drug Deliv Rev*. 2004;56:1127–1141.
24. Pan D, Turner JL, Wooley KL. Folic acid-conjugated nanostructured materials designed for cancer cell targeting. *Chem Commun*. 2003; 19:2400–2401.
25. Dixit V, Van den Bossche J, Sherman DM, Thompson DH, Andres RP. Synthesis and grafting of thioctic acid-PEG-folate conjugates onto Au nanoparticles for selective targeting of folate receptor-positive tumor cells. *Bioconjug Chem*. 2006;17:603–609.
26. Sudimack J, Lee RJ. Targeted drug delivery via the folate receptor. *Adv Drug Deliv Rev*. 2000;41:147–162.
27. Lee ES, Na K, Bae YH. Polymeric micelle for tumor pH and folate-mediated targeting. *J. Controlled Release*. 2003;91:103–113.
28. Mu L, Feng SS. Vitamin E TPGS used as emulsifier in the solvent evaporation/extraction technique for fabrication of polymeric nanospheres for controlled release of paclitaxel (Taxol (R)). *J Control Release*. 2002;80:129–144.
29. Dou HJ, Jiang M, Peng HS, Chen DY, Hong Y. pH-dependent self-assembly: micellization and micelle-hollow-sphere transition of cellulose-based copolymers. *Angew Chem Int Ed*. 2003;42:1516–1519.

Manuscript received Apr. 29, 2013, and revision received Jun. 26, 2013.